

Properties of holographic dark energy at the Hubble length

Ivan Duran and Luca Parisi

Abstract We consider holographic cosmological models of dark energy in which the infrared cutoff is set by the Hubble's radius. We show that any interacting dark energy model, regardless of its detailed form, can be recast as a non interacting model in which the holographic parameter c^2 evolves slowly with time. Two specific cases are analyzed. We constrain the parameters of both models with observational data, and show that they can be told apart at the perturbative level.

1 Introduction

Whatever the nature of DE it seems reasonable that it fulfills the holographic principle [1]. Based on this, Li [2] proposed for the density of DE the expression

$$\rho_X = \frac{3M_P^2 c^2}{L^2}. \quad (1)$$

where c^2 is a dimensionless parameter and L the IR cutoff.

We will take L as the Hubble radius, $L = H^{-1}$, see e.g. [3]. See e.g. [2, 4, 5, 6, 7] for other choices. It has been argued that an IR cutoff defined by H^{-1} cannot lead to an accelerated Universe. However, if DM and DE interact according to

$$\dot{\rho}_M + 3H\rho_M = Q \quad \text{and} \quad \dot{\rho}_X + 3H(1+w)\rho_X = -Q, \quad (2)$$

where $Q > 0$ is the interaction term, an accelerated expansion can be achieved [8].

Ivan Duran
Universitat Autònoma de Barcelona, e-mail: ivan.duran@uab.cat

Luca Parisi
Università di Salerno, e-mail: parisi@sa.infn.it

In [9] the c^2 parameter was considered to increase slowly with time in such a way that $0 < (\dot{c}^2) \leq H$. In what follows, quantities referring to models with variable c^2 will be noted by a tilde. By assumption their energy densities conserve separately,

$$\dot{\tilde{\rho}}_M = -3H\tilde{\rho}_M \quad \text{and} \quad \dot{\tilde{\rho}}_X = -3H(1 + \tilde{w})\tilde{\rho}_X. \quad (3)$$

By considering both points of view it was demonstrated that identical backgrounds evolutions can be described by an interacting holographic DE model, with c^2 strictly fixed, or by a non-interacting holographic DE model in which \tilde{c}^2 depends weakly on time [10]. In spite that the global evolution is identical in both scenarios, the energy densities and the EoS parameters can behave rather differently.

2 Proposed models: model 1 and model 2

Here we consider the holographic interacting model studied in [11] in order to construct its equivalent $\tilde{c}^2(t)$ model. In the former the IR cutoff was also set by the Hubble's length and the interaction term was $Q \equiv 3AH_0\rho_M$, with A a semipositive definite constant, related to the constant decay rate of DE into DM, Γ , by $A \equiv \frac{\Gamma}{3H_0r}$, with $r \equiv \rho_M/\rho_X$. Thus, the Hubble function takes the form

$$H = H_0 \left(A + (1 - A)(1 + z)^{\frac{3}{2}} \right), \quad (4)$$

We expand $H^2(z)$ assuming that the $(1 + z)^3$ term corresponds to DM and identify the remainder of the expression as the DE energy density. Thus,

$$\frac{M_P^{-2}}{3H_0^2} \tilde{\rho}_M = (1 - A)^2 (1 + z)^3 \quad \text{and} \quad \frac{M_P^{-2}}{3H_0^2} \tilde{\rho}_X = A^2 + 2A(1 - A)(1 + z)^{\frac{3}{2}}, \quad (5)$$

alongside with

$$\tilde{c}^2 = \frac{2A(1 - A)(1 + z)^{\frac{3}{2}} + A^2}{\left(A + (1 - A)(1 + z)^{\frac{3}{2}} \right)^2}. \quad (6)$$

The best fit values are found to be $H_0 = 69.4 \pm 1.7$ and $A = 0.588 \pm 0.004$, while $\chi^2/dof = 1.00$. For details see [10]. As the top right panel of Fig. 1 shows, the coincidence problem (i.e., “why the densities of DM and DE are of the same order precisely today?”) gets solved (r stays constant) in the interacting case (solid green line). In the \tilde{c}^2 model (thin dot-dashed red lines) it is not solved but results much less severe than in Λ CDM (thick short dashed blue line).

We next propose model 2. In this model DM and DE evolve separately but \tilde{c}^2 varies slowly with time. In order to have $0 \leq \tilde{c}^2 \leq 1$, and $(\tilde{c}^2)' \geq 0$ we define

$$\tilde{c}^2 = \frac{1}{1 + \tilde{r}_0(1 + z)^\epsilon} \quad (7)$$

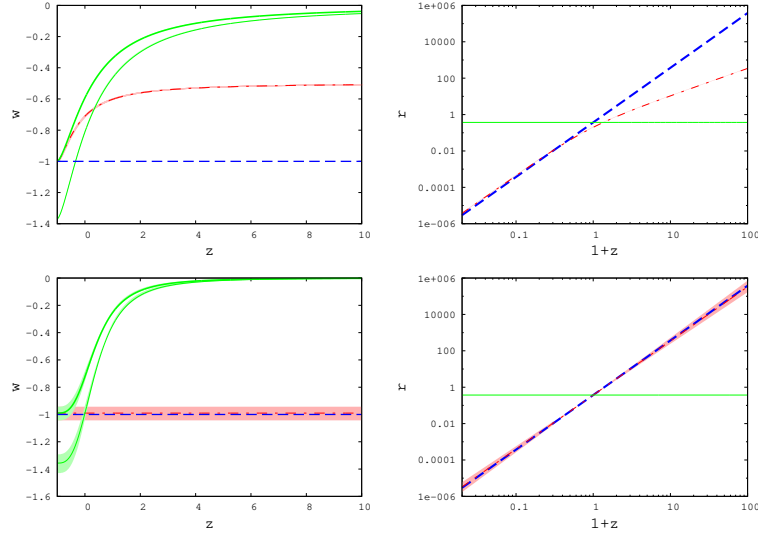


Fig. 1 Top panels are for model 1 and bottom panels for model 2. Left panels: EoS parameter for the the interacting (w thin line, and w_{eff} thick line), the c^2 and Λ CDM models. Right panels: energy densities ratios, $r \equiv \rho_M/\rho_X$, versus $1+z$ for the Λ CDM, the interacting and the c^2 models. Solid (green) lines are used for the interacting case, thin dot dashed (red) lines for the c^2 model, and thick short dashed (blue) for Λ CDM.

where $\tilde{r}_0 \equiv \frac{\tilde{\Omega}_{M0}}{\Omega_{X0}}$ and ε a semipositive definite constant. In this case

$$H = H_0 \sqrt{\tilde{\Omega}_{M0}(1+z)^3 + \tilde{\Omega}_{X0}(1+z)^{3-\varepsilon}} \quad (8)$$

is identical to a spatially flat w CDM model with $\tilde{w} = -\frac{\varepsilon}{3}$. If we consider Eq.(8) as resulting from some interaction between DE and DM, the interacting term would be

$$Q = -3c^2 w \rho_M H, \quad (9)$$

Detailed calculations can be found in [10]. The best fit values are $\Omega_{X0} = 0.73 \pm 0.007$, $H_0 = 71.5 \pm 2.6$ and $\varepsilon = 2.97^{+0.16}_{-0.14}$, being $\chi^2/dof = 0.97$. As the bottom right panel of Fig. 1 shows the interacting model (solid green line) solves the coincidence problem.

3 Evolution of the subhorizon perturbations

In the interacting case, the energy-momentum tensors of DM and DE are not independently conserved, $T_i^{\mu\nu}{}_{;\mu} = Q_i^\nu$. For subhorizon scales, i.e., $k \gg aH$, the density and energy and momentum conservation equations simplify to

$$\dot{\delta}_M = -\frac{\theta_M}{a} \quad \text{and} \quad \dot{\theta}_M = -H\theta_M + \frac{k^2}{a}\phi \quad (10)$$

$$\dot{\delta}_X = -(1+w)\frac{\theta_X}{a} - 3H(1-w)\delta_X + \frac{1}{\rho_X}(Q\delta_X - \delta Q), \quad (11)$$

$$\dot{\theta}_X = \frac{1}{(1+w)}\frac{k^2}{a}\delta_X - \frac{Q}{(1+w)\rho_X}(\theta_M - 2\theta_X), \quad (12)$$

See [10] for the description of the δQ in each model. To confront it with observations, we resort to the growth function, $f \equiv d \ln \delta_M / d \ln a$ [12]. We can see in Fig. 2, that matter density perturbations clearly differ in the interacting and the \tilde{c}^2 scenarios.

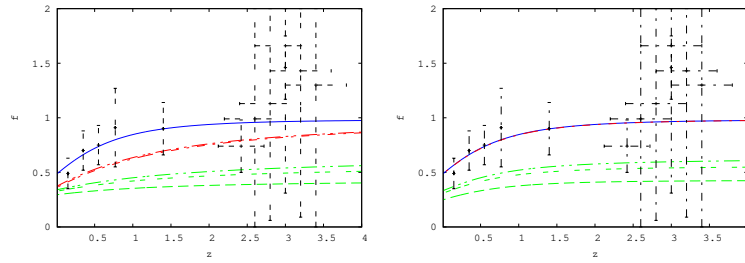


Fig. 2 Left panel: evolution of the growth function, f , versus redshift for model 1. Right panel: the same for model 2. The dashed (green) lines describe the interacting scenario, the dot-dashed (red) lines the \tilde{c}^2 , and the solid (blue) line the Λ CDM. The observational data were borrowed from [13].

Acknowledgements We are indebted to Diego Pavón, Gaetano Vilasi, Ninfa Radicella and Fernando Atrio-Barandela for fruitful discussions. ID was supported by the Spanish MICINN under Grant No. FIS2009-13370-C02-01, by the Generalitat de Catalunya under Grant No. 2009SGR-00164. LP was partially supported by the Italian MIUR through the PRIN 2008 grant.

References

1. G. 't Hooft, “Dimensional reduction in quantum gravity”, preprint gr-qc/9310026; L. Susskind, J. Math. Phys. (N.Y.) **36**, 6377 (1995).
2. M. Li, Phys. Lett. B **603**, 1 (2004).
3. S. D. H. Hsu, Phys. Lett. B **594**, 13 (2004); D. Pavón and W. Zimdahl, Phys. Lett. B **628**, 206 (2005).
4. C. Gao, F. Wu, X. Chen, and Y.G. Shen, Phys. Rev. D **79**, 043511 (2009).
5. L. Xu, W. Li, and J. Lu, Mod. Phys. Lett. A **24**, 1355 (2009).
6. M. Suwa, T. Nihei, Phys. Rev. D **81**, 023519 (2010).
7. I. Duran and D. Pavón, Phys. Rev. D **83**, 023504 (2011).
8. W. Zimdahl and D. Pavón, Class. Quantum Grav. **24**, 5461 (2007).
9. D. Pavón, W. Zimdahl, Phys. Lett. B **628**, 206 (2005).
10. I. Duran and L. Parisi, Phys. Rev. D **85**, 123538 (2012).
11. I. Duran, D. Pavón and W. Zimdahl, JCAP **07**, 018 (2010).
12. L. Wang and P. J. Steinhardt, Astrophys. J. **508**, 483 (1998).
13. Y. Gong, Phys. Rev. D **78**, 123010 (2008).